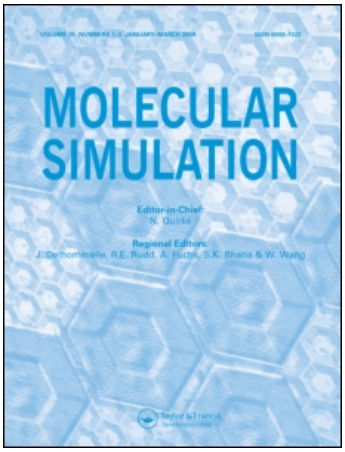

Molecular Simulation
Publication details, including instructions for authors and subscription information:
http://www.informaworld.com/smpp/title~content=t713644482

Atomistic simulation of dislocation interactions in a model crystal subjected to shear

M. Popova[a]; Y. -L. Shen[a]; T. A. Khraishi[a]
[a] Department of Mechanical Engineering, University of New Mexico, Albuquerque, NM, USA

To cite this Article Popova, M. , Shen, Y. -L. and Khraishi, T. A.(2005) 'Atomistic simulation of dislocation interactions in a model crystal subjected to shear', Molecular Simulation, 31: 14, 1043 — 1049
To link to this Article: DOI: 10.1080/08927020500349999
URL: http://dx.doi.org/10.1080/08927020500349999

Molecular Simulation, Vol. 31, No. 14–15, 15–30 December 2005, 1043–1049

Taylor & Francis
Taylor & Francis Group

Atomistic simulation of dislocation interactions in a model crystal subjected to shear

M. POPOVA, Y.-L. SHEN* and T.A. KHRAISHI

Department of Mechanical Engineering, University of New Mexico, Albuquerque, NM 87131, USA

(Received September 2005; in final form September 2005)

The interaction of edge dislocations in a two-dimensional (2D) model crystal subjected to "simple shear" is studied using molecular statics simulations. An initial point defect is introduced in the model to trigger the dislocation activities in a controlled manner. We consider dislocations gliding towards one another on parallel slip planes separated by various distances. The overall load-displacement response of the crystal is obtained from the simulations, which can be correlated with the nano-scale atomistic mechanisms. Although the crystal is inherently anisotropic, the incipient dislocation plasticity is such that slip is parallel to the primary shear direction as clearly demonstrated in this work. It is also illustrated that dislocation annihilation, as well as dislocation encounter which leaves behind a point defect, can be unambiguously modeled. Throughout the deformation history, more dislocations capable of gliding in the crystal tend to generate a weaker mechanical response and more pronounced plasticity. The present study also offers mechanistic insight into experimentally observed small-scale crystal plasticity.

Keywords: Atomistic simulation; Dislocation; Crystal; Nano-scale plasticity

1. Introduction

The interaction of dislocations in metallic crystals plays a central role in determining the mechanical properties. Continuum-based dislocation theory offers a mechanistic basis for predicting and analyzing forces acting on individual dislocations and their resulting movement [1,2]. On the more elementary side, conceptual illustrations have long been employed for elucidating simple cases of dislocation interactions. For example, two parallel edge dislocations of opposite sign on the same slip plane tend to attract one another, resulting in annihilation [3]. In discrete dislocation dynamics simulations, this type of short-range interaction typically disturbs the seamless flow of the rest of the computation [4–7]. The detailed atomistic characteristics involved in the interaction can naturally be analyzed only using molecular level modeling. While large-scale molecular simulations are extensively utilized for studying complicated microscopic features [8–15], in this report, we present a small-scale two-dimensional (2D) atomistic analysis of interaction between edge dislocations in a model crystal. The primary objective is to employ a simple modeling strategy for gaining fundamental insight into nano-scale defect mechanisms. Attention is also focused on correlating the atomic level dislocation activities with the overall mechanical response of the material.

2. Modeling approach

Figure 1(a) shows the model system, which is a close-packed planar crystal with one of its close-packed directions parallel to the x-axis. To assist in triggering the onset of crystal plasticity, an artificial defect, in the form of a self-interstitial, is introduced in the model (circa $x = 130\,\text{Å}$ and $y = 45\,\text{Å}$) and allowed to equilibrate with its surrounding atoms before the loading steps commence. This technique enables elastic–plastic transition and the underlying atomistic processes to be simulated with the simple pair-potential adopted here [16,17]. The Morse interatomic potential is used with the parameters determined by fitting to experimental data of the equilibrium lattice parameter, cohesive energy and bulk modulus of copper featuring near-neighbor interactions [18,19]. The molecular statics simulation of shear loading is carried out by prescribing a small displacement in the x-direction on the top boundary atoms at each step while

*Corresponding author. Email: shenyl@me.unm.edu

Molecular Simulation
ISSN 0892-7022 print/ISSN 1029-0435 online © 2005 Taylor & Francis
http://www.tandf.co.uk/journals
DOI: 10.1080/08927020500349999

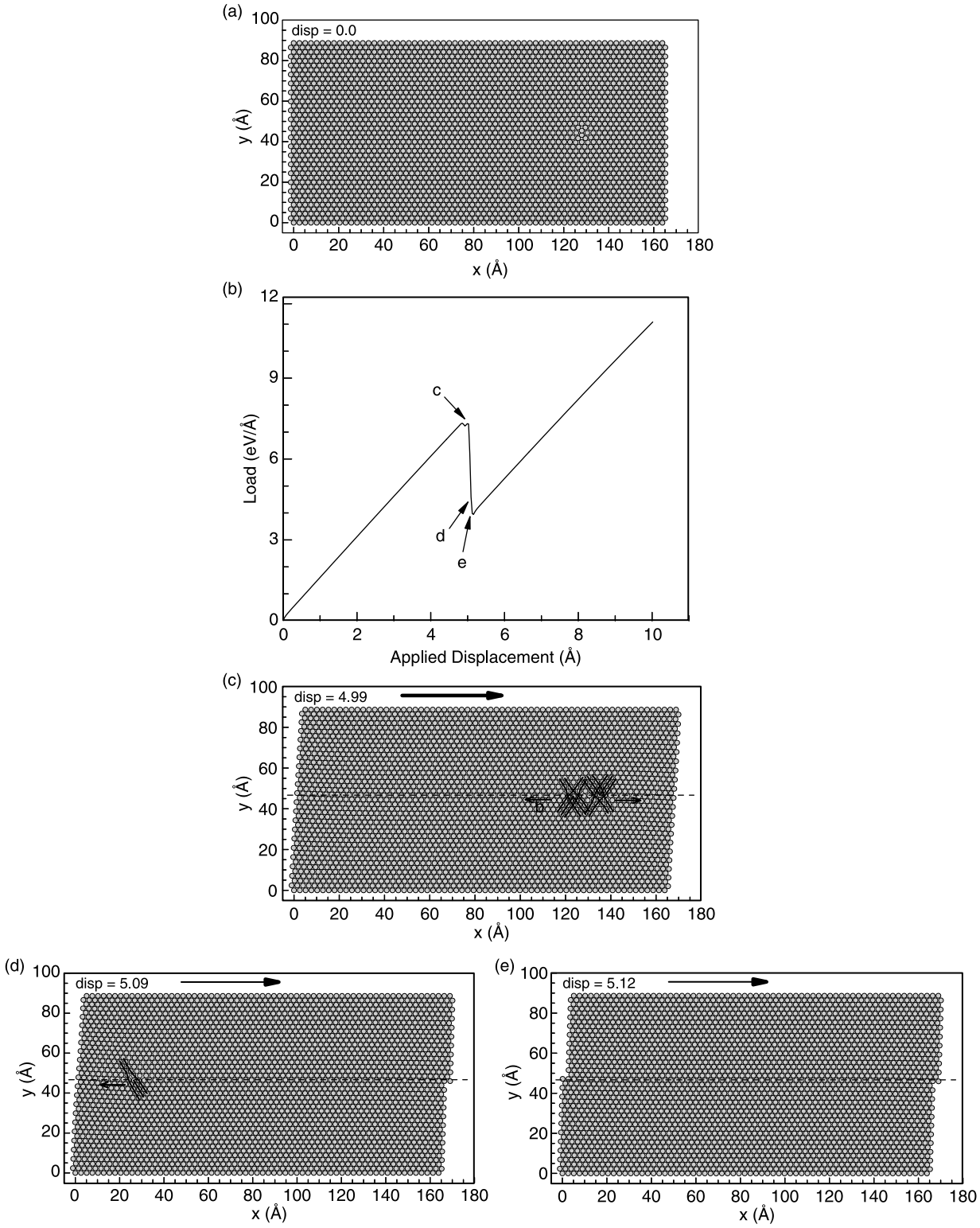

Figure 1. (a) Atomic configuration of the model crystal containing one initial self-interstitial before loading. (b) Simulated overall shear load-displacement curve. (c)–(e) Snapshots of atomic positions corresponding to points c–e, respectively, along the load-displacement curve shown in (b).

fixing the positions of the bottom boundary atoms. The *y*-positions of the top boundary atoms are kept unchanged. (This process is termed "simple shear" as opposed to "pure shear"). The movement of the side boundary atoms is not restricted. In response to each loading step the atomic points are allowed to iteratively reach their new equilibrium positions. The overall shear force is calculated by summing the *x*-component forces along the top boundary atoms where the displacement is prescribed.

Figure 1(b) shows the overall load-displacement curve resulting from the simulation. Since our focus is on correlating the dislocation behavior with the overall response, the curve in figure 1(b) is shown only up to a nominal shear strain of about 6%. It can be seen that the elastic response is interrupted by a sudden large-scale reduction in load. Figure 1(c)–(e) show the snapshots of atomic positions corresponding to the points c–e, respectively, labeled along the load-displacement history in figure 1(b). The distorted crystal shape can be clearly seen. In figure 1(c), the dislocation dipole evolving from the interstitial is already discernable, and is highlighted with some line segments in an elementary manner. Depending on the view angle, each dislocation can be conveniently identified with two different "extra half planes" as indicated. However, a simple Burgers circuit operation will confirm that it is an edge dislocation with an effective extra half plane oriented vertically, with the Burgers vector parallel to the x-direction. The slip plane is indicated by the dashed horizontal line. In response to the applied shear, the left dislocation (negative edge) will glide to the left and the right dislocation (positive edge) will glide to the right. In all subsequent figures, we only highlight each dislocation with one set of slant extra half plane for the purpose of clarity.

In figure 1(d), which is during the reduction in load (figure 1(b)), it is seen that the right dislocation has moved out of the right-hand boundary and created a slip step, while the left dislocation is now close to the left-hand boundary. In figure 1(e), which corresponds to the bottom point of the load reduction (figure 1(b)), the left dislocation has also moved out and created a slip step. There is a permanent shape change of the crystal, which signifies plastic yielding, and the crystal now contains no defect. Therefore, an elastic response takes over beyond point e in figure 1(b). The sharp load reduction in the load-displacement curve is associated with the extensive movement of dislocations and the creation of slip steps at the free surface.

Since our primary objective is to examine the interaction of dislocations, a second initial self-interstitial is placed in the model in all the simulations presented below. One dislocation resulting from each initial defect will tend to glide towards the center of the crystal and encounter the other incoming one. The two interstitials have the original x-positions near $x = 35$ and 130 Å. However, several cases of different y-positions are considered, giving rise to the approaching dislocations gliding along different slip planes, as detailed in the following section.

3. Results and discussion

We consider four scenarios, differed by the relative y-positions of the two dislocations approaching one another, as shown schematically in the insets of figures 2(a)–5(a). The other two dislocations, moving directly towards the right-hand and left-hand free surfaces of the crystal, are not included in the insets. In case 1 (figure 2(a)), the two dislocations are gliding on slip planes two atomic distances apart, with the positive edge dislocation (initially at left) being in a lower position. In case 2 (figure 3(a)), the positive and negative edge dislocations are at exactly the same slip planes. In case 3 (figure 4(a)), the slip planes of the positive and negative edge dislocations are separated by one atomic layer. In case 4 (figure 5(a)), the slip plane of the positive edge dislocation is several atomic distances higher than that of the negative edge dislocation. The overall load-displacement curves for these four cases are also shown in figures 2(a)–5(a). Several points (b,c,d, etc.) are labeled along the curves, with the atomic snapshots shown in the respective parts of the figures.

In figure 2(a), the load-displacement curve shows two large-scale reductions in load. At point b (figure 2(b)) where the crystal is still undergoing initial elastic deformation, two pairs of dislocations are being formed from the initial defect sites. The first load reduction is associated with the dislocations moving over a large distance, figure 2(c), and with two of them later moving out of the crystal to create slip steps, figure 2(d). In figure 2(c), the two inner dislocations are very close to each other. Although they have their own strain fields, the modeling setup is such that the imposed shear deformation dominates the process and continues to drive the dislocations in their respective directions so, in figure 2(d), they have just glided past one another. Beyond point d, a brief elastic response ensues, with the two dislocations being relatively stagnant (i.e. in near quasi-static equilibrium under the current configuration and loading). The second large-scale reduction in load appears when the dislocations are able to move over a large distance, figure 2(e), and eventually out of the crystal to create further slip steps, figure 2(f). Beyond the bottom point of the second load reduction, there is no defect left in the crystal so the material becomes elastic again.

It is observed by comparing the cases of figures 1 and 2 that, one initial point defect in the crystal results in two dislocations and eventual two slip steps with one significant load reduction in the overall material response. When there are two initial point defects, a total of four dislocations are created, leading to eventual four slip steps with two significant load reductions in the load-displacement curves.

Figure 3 shows the case where the two inner dislocations glide on the same plane. Figure 3(b) and (c) shows the atomic snapshots during the sudden load reduction observed in figure 3(a). In figure 3(b), all four dislocations (evolved from the two initial defects) are still gliding inside the crystal. In figure 3(c), the leftmost dislocation has moved out and created a slip step and the rightmost one is now very close to the free surface. The two inner dislocations seen in figure 3(b), however, have now combined and become annihilated and can no longer be seen in figure 3(c). Therefore, aside from

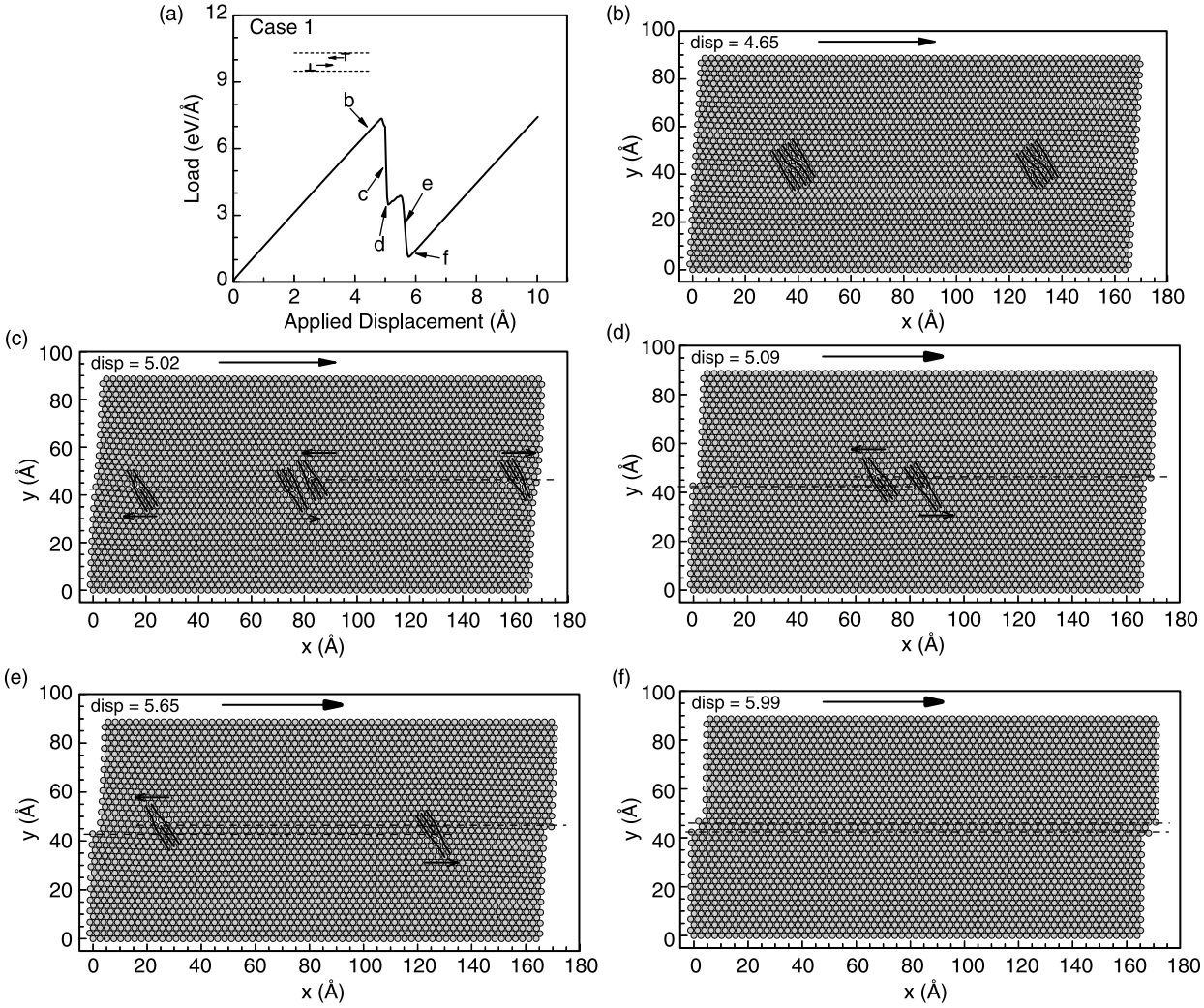

Figure 2. (a) Simulated overall load-displacement curve for case 1, with the schematic of interacting dislocations shown in the inset. (b)–(f) Snapshots of atomic positions corresponding to points b–f, respectively, along the load-displacement curve in (a).

the outgoing dislocation, there is no other defect left in the crystal at this stage. When the load reaches minimum at the end of the reduction (point d in figure 3(a)), the crystal is free of dislocations and there is one slip step on each free surface. A comparison of the cases of figures 2 and 3 reveals that the annihilation of two dislocations results in two fewer slip steps created at the free surfaces and one fewer sudden reduction in load of the overall material response. In other words, fewer mobile dislocations in the crystal will give rise to a stronger material (or a smaller extent of plastic deformation). It is noted that the overall load-displacement curve in figure 3(a) appears to be identical to that in figure 1(b) although the two cases have different defect configurations. This is apparently due to the model setup which results in the annihilation of dislocations.

Figure 4 considers a case slightly different from that of figure 3, with the slip planes of interest being separated by one layer of atoms. Here we present three snapshots of atomic positions, namely points b–d along the load-displacement curve shown in figure 4(a). At point b (figure 4(b)), which is at the beginning stage of the load reduction, the two pairs of dislocations have evolved and are gliding along their slip planes. In figure 4(c), which is during the load reduction, the two outgoing dislocations are near the free surfaces, and the inner two have already combined. Due to the fact that there is a layer of atoms between the slip planes of the two interacting dislocations, it is impossible to have a complete annihilation but a vacancy is left at the spot where the two dislocations encountered. At the end of the load reduction, figure 4(d), two slip steps have been formed and the vacancy remains in the crystal. Further deformation results in essentially an elastic response, as seen in figure 4(a).

It is worth mentioning that the vacancy left in figure 4(d) will eventually disappear ("closed" by the adjacent atoms) with further shear deformation, although this is beyond the scope of the present paper and is not shown here. In a previous atomistic study of uniaxial tensile loading, however, a vacancy tends to nucleate more dislocations and later evolves into a growing void, leading to ductile failure [16].

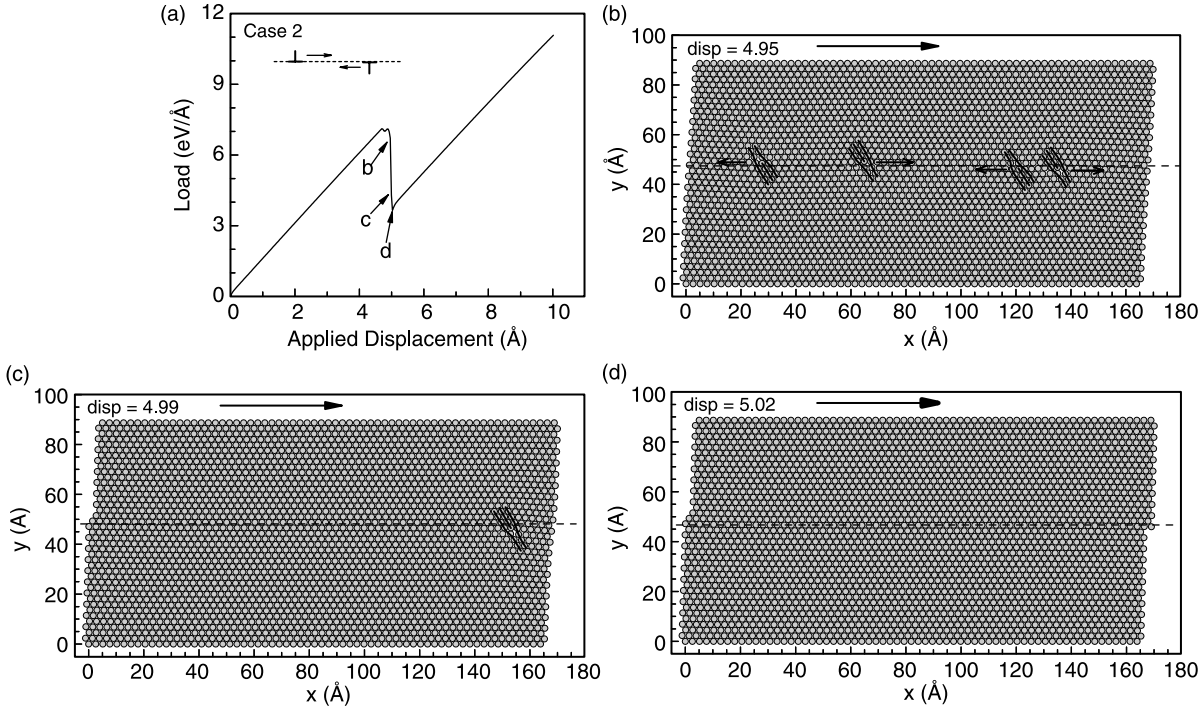

Figure 3. (a) Simulated overall load-displacement curve for case 2, with the schematic of interacting dislocations shown in the inset. (b)–(d) Snapshots of atomic positions corresponding to points b–d, respectively, along the load-displacement curve shown in (a).

Figure 5 is for the case where the two interacting dislocations glide on planes farther apart, with the positive edge dislocation being at a higher position. At point b (figure 5(b)), the two pairs of dislocations have formed and started to move. The dislocations have slipped in response to the applied shear as evidenced in figure 5(c). At the end of the first large-scale load reduction, figure 5(d), the two outside dislocations have slipped out of the crystal but

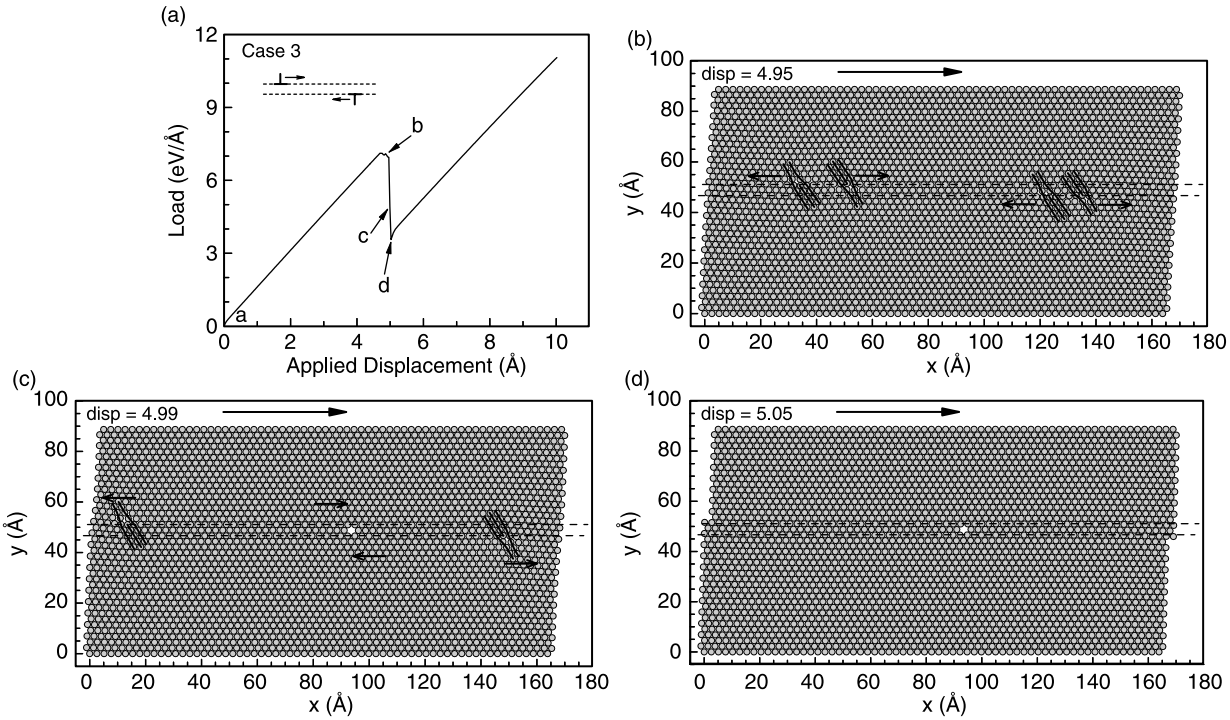

Figure 4. (a) Simulated overall load-displacement curve for case 3, with the schematic of interacting dislocations shown in the inset. (b)–(d) Snapshots of atomic positions corresponding to points b–d, respectively, along the load-displacement curve shown in (a).

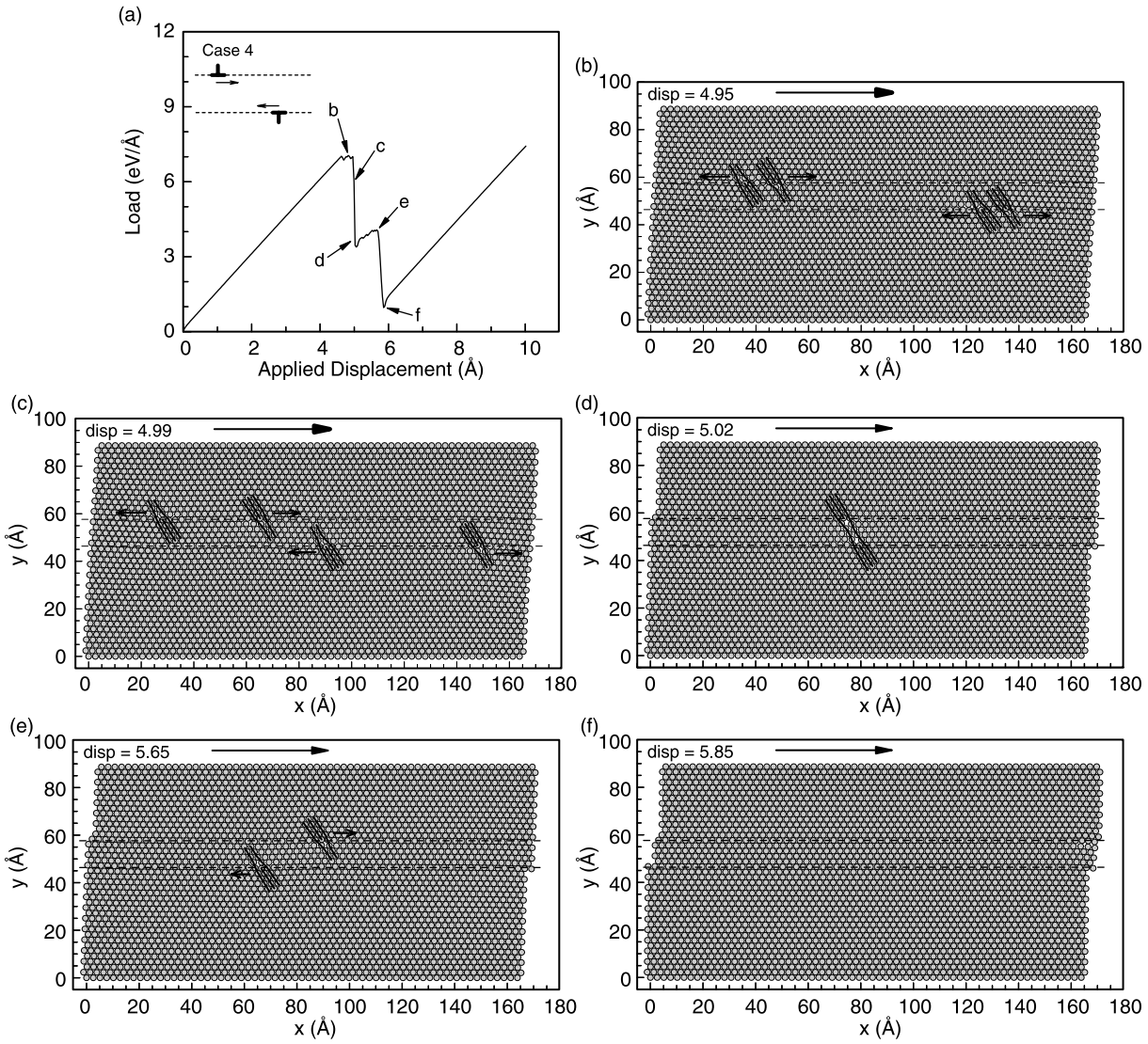

Figure 5. (a) Simulated overall load-displacement curve for case 4, with the schematic of interacting dislocations shown in the inset. (b)–(f) Snapshots of atomic positions corresponding to points b–f, respectively, along the load-displacement curve in (a).

the inner two remain. There appears to be a possibility to form multiple vacancies since the local structure is somewhat "opened". However, the distance between the two dislocations still dictates that the atoms in between are largely bonded. From points d to e in the load-displacement curve in figure 5(a), the dislocations become separated due to the dominance of applied shear deformation, as observed in figure 5(e). Figure 5(f) shows that these two dislocations have moved out of the crystal to create a pair of slip steps. As a consequence, a second load reduction from points e to f appears in figure 5(a). Beyond point f the crystal is free of defects and an elastic response resumes.

In the last case (figure 5), since all four dislocations remained in the crystal before slipping out, there were eventually four slip steps created and there were two large load reductions in the load-displacement curve, which is qualitatively similar to the case considered in figure 2. Overall, the material is weaker upon plastic yielding (i.e. the overall load becomes small after the two load reductions).

Although the focus of this study is on the 2D illustrations of dislocation activities and their correlation with the overall material response, the results also provide some insight into strengthening and small-scale plasticity phenomena of single crystals, which are currently of widespread interest. For instance, experiments have shown unusually high flow stresses of specially prepared small crystals [20,21], which was attributed to "dislocation starvation" after available dislocations have moved out of the crystal. In the present work, we have shown the material strength started to increase once the dislocations have moved out of the crystal. In addition, fewer mobile dislocations throughout the deformation history (figures 1, 3 and 4) would lead to generally stronger response than the cases of more mobile dislocations existent in the crystal (figures 2 and 5). Therefore, the simulations have offered a mechanistic

rationale, albeit qualitatively, for the experimental observations.

4. Conclusions

We have employed molecular statics simulations to examine the interaction between dislocations in a model 2D crystal having a close-packed crystal structure, under the simple shear loading. The correlation between the atomistic mechanisms and the overall material response was also explored. It is shown that dislocation annihilation can be unambiguously modeled. The simulation also illustrated the possibility of dislocation encounter which leaves behind a point defect (vacancy). When the slip planes of two approaching dislocations are several atomic planes apart, they tend to glide past one another in response to the imposed shear deformation at the crystal boundary. Macroscopic load-displacement curves are obtained from the simulations in a straightforward manner, which shows correspondence with the nano-scale dislocation activities. Under the displacement controlled deformation, a sudden reduction in overall load is associated with the mobile dislocations moving over a significant distance and then out of the crystal to create slip steps at the free surface. During the deformation history, more dislocations capable of gliding in the crystal will lead to a generally weaker mechanical response and more pronounced plasticity. The simulations also provide a mechanistic rationale for the "dislocation starvation" mechanism used for explaining small-scale plasticity phenomena observed in recent experiments.

Acknowledgements

This work was supported by Air Force Office of Scientific Research under grants F49620-01-1-0565 and FA9550-05-1-0033.

References

[1] J.P. Hirth, J. Lothe. *Theory of Dislocations*, John Wiley & Sons, New York (1982).
[2] D. Hull, D.J. Bacon. *Introduction to Dislocations*, Butterworth-Heinemann, Woburn, UK (1984).
[3] W. Hayden, W.G. Moffat, J. Wulff. *Structure and Properties of Materials*, III, p. 75, John Wiley & Sons, New York (1965).
[4] M. Rhee, H.M. Zbib, J.P. Hirth, H. Huang, T. de la Rubia. Models for long-/-short-range interactions and cross slip in 3D dislocation simulation of BCC single crystals. *Model. Simul. Mater. Sci. Eng.*, **6**, 467 (1998).
[5] B. von Blanckenhagen, E. Arzt, P. Gumbsch. Discrete dislocation simulation of plastic deformation in metal thin films. *Acta Mater.*, **52**, 773 (2004).
[6] L.P. Kubin, G. Canova, M. Condat, B. Devincre, V. Pontikis, Y. Brechet. Dislocation microstructures and plastic flow: a 3D simulation. *Solid State Phenom.*, **23-24**, 455 (1992).
[7] A. Needleman. Computational mechanics at the mesoscale. *Acta Mater.*, **48**, 105 (2000).
[8] M.F. Horstemeyer, M.I. Baskes, A. Godfrey, D.A. Hughes. A large deformation atomistic study examining crystal orientation effects on the stress–strain relationship. *Int. J. Plast.*, **18**, 203 (2002).
[9] H. Van Swygenhoven, P.M. Derlet, A. Hasnaoui. Atomistic modeling of strength of nanocrystalline metals. *Adv. Eng. Mater.*, **5**, 345 (2003).
[10] E.T. Lilleodden, J.A. Zimmerman, S.M. Foiles, W.D. Nix. Atomistic simulations of elastic deformation and dislocation nucleation during nanoindentation. *J. Mech. Phys. Sol.*, **51**, 901 (2003).
[11] V. Yamakov, D. Wolf, S.R. Phillpot, H. Gleiter. Grain-boundary diffusion creep in nanocrystalline palladium by molecular-dynamics simulation. *Acta Mater.*, **50**, 61 (2002).
[12] J. Li, A.H.W. Ngan, P. Gumbsch. Atomistic modeling of mechanical behavior. *Acta Mater.*, **51**, 5711 (2003).
[13] A. Latapie, D. Farkas. Molecular dynamics investigation of the fracture behavior of nanocrystalline alpha-Fe. *Phys. Rev. B*, **69**, 134110 (2004).
[14] B.J. Lee, B.D. Wirth, J.H. Shim, J. Kwon, S.C. Kwon, J.H. Hong. Modified embedded-atom method interatomic potential for the Fe-Cu alloy system and cascade simulations on pure Fe and Fe–Cu alloys. *Phys. Rev. B*, **71**, 184205 (2005).
[15] J.D. Schall, D.W. Brenner. Atomistic simulation of the influence of pre-existing stress on the interpretation of nanoindentation data. *J. Mater. Res.*, **19**, 3172 (2004).
[16] Y.-L. Shen. On the atomistic simulation of plastic deformation and fracture in crystals. *J. Mater. Res.*, **19**, 973 (2004).
[17] Y.-L. Shen. Strength and interface-constrained plasticity in thin metal films. *J. Mater. Res.*, **18**, 2281 (2003).
[18] R. Phillips. *Crystals, Defects and Microstructures—Modeling Across Scales*, p. 206, Cambridge University Press, Cambridge (2001).
[19] P.M. Morse. Dynamic molecules according to the wave mechanics. II. Vibrational levels. *Phys. Rev.*, **34**, 57 (1929).
[20] M.D. Uchic, D.M. Dimiduk, J.N. Florando, W.D. Nix. Sample dimensions influence strength and crystal plasticity. *Science*, **305**, 986 (2004).
[21] J.R. Greer, W.C. Oliver, W.D. Nix. Size dependence of mechanical properties of gold at the micron scale in the absence of strain gradients. *Acta Mater.*, **53**, 1821 (2005).